Eur. Phys. J. C (2026) 86:392
https://doi.org/10.1140/epjc/s10052-026-15641-z

THE EUROPEAN PHYSICAL JOURNAL C

Regular Article - Theoretical Physics

Dipolar magnetic field by static current loop in exponential metric

Bobur Turimov[1,2,3,a], **Bekzod Rahmatov**[4,5,b], **Zikrilla Yasakov**[6,c], **Yunus Turaev**[7,d], **Sulton Usanov**[8,e], **Zebo Avezmuratova**[9,f], **Azamat Japakov**[10,g]

[1] Engineering School, Central Asian University, Milliy bog Str.264, 111221 Tashkent, Uzbekistan
[2] University of Tashkent for Applied Sciences, Gavhar Str.1, 100149 Tashkent, Uzbekistan
[3] Ulugh Beg Astronomical Institute, Astronomy St. 33, Tashkent 100052, Uzbekistan
[4] New Uzbekistan University, Movarounnahr Str.1, Tashkent 100000, Uzbekistan
[5] Tashkent State Technical University, Tashkent 100095, Uzbekistan
[6] Samarkand State University of Architecture and Construction, Lolazor Street 70, 140147 Samarkand, Uzbekistan
[7] Mamun University, Bol-Khovuz Str. 2, 220900 Khiva, Uzbekistan
[8] Kimyo International University in Tashkent, Shota Rustaveli Str.156, 100121 Tashkent, Uzbekistan
[9] Department of Physics and Astronomy, Urgench State Pedagogical Institute, Gurlan Str.1-A, 220100 Urgench, Uzbekistan
[10] Urgench State University named after Abu Rayhan Biruni, Kh. Olimjon Str.14, 220100 Urgench, Uzbekistan

Received: 3 October 2025 / Accepted: 1 April 2026

Abstract We investigated the dipolar magnetic field generated by a static current loop around a compact gravitational source described by the exponential metric. Starting from Maxwell's equations, we derived the expression for the electromagnetic vector potential in this spacetime and obtained analytical solutions. The angular dependence of the vector potential is expressed through Legendre polynomials, while the radial part is represented by the hypergeometric function of the first kind. The integration constants were determined by enforcing the continuity of the vector potential at the location of the source and by substituting the solution back into Maxwell's equations. The resulting magnetic field is uniform in the interior region, resembling the Wald solution, whereas in the exterior region it assumes a dipolar structure. Moreover, the external magnetic field strength decreases with increasing radial distance. We have investigated the effect of introducing a dipole magnetic field on the motion of charged particles around the compact object. Our results show that the presence of this magnetic field alters the particle dynamics and causes the radius of the innermost stable circular orbit (ISCO) to move outward compared with the case of a neutral particle.

1 Introduction

Magnetic fields surrounding black holes represent a fundamental aspect of astrophysics, particularly in the vicinity of rotating black holes and neutron stars. These fields are not intrinsic properties of the black holes themselves but are mainly generated by the surrounding accretion disk material. Investigating magnetic fields in strong gravity regimes is crucial, since the interplay between intense gravitational forces and electromagnetic fields strongly influences accretion dynamics, jet formation, and the long-term evolution of compact objects. Recent observational advances, most notably those from the Event Horizon Telescope (EHT), have enabled direct probing of magnetic field signatures near the event horizon, providing new insights into their structure and astrophysical effects [1].

Investigating electromagnetic phenomena near black holes involves solving the complex Einstein–Maxwell equations, a significant mathematical challenge. The simplest exact solutions to these equations include the Melvin universe [2] and the Reissner–Nordström metric [3]. In many astrophysical scenarios, electromagnetic fields are weak enough that they do not significantly affect spacetime geometry, allowing Maxwell's equations to be solved on a fixed background metric. For instance, Wald's model [4] considers a black hole

[a] e-mail: bturimov@astrin.uz
[b] e-mail: rahmatovbekzod@samdu.uz (corresponding author)
[c] e-mail: zikrillo87@mail.ru
[d] e-mail: yunus.turaev.nw@gmail.com
[e] e-mail: sm.usanov@kiut.uz
[f] e-mail: zeboavezmuratova1981@mail.ru
[g] e-mail: azamat@urdu.uz

Published online: 19 April 2026

immersed in a uniform magnetic field. Numerical simulations also show that when magnetized stars collapse into black holes, they can pass their magnetic fields to the new black hole, highlighting the critical role of magnetic fields in black hole astrophysics [5].

Comprehending magnetic fields is essential for understanding black hole growth, their interactions with surrounding environments, and the formation of relativistic jets that significantly affect host galaxies. For example, magnetic field strengths can reach approximately $\sim 10^8$ G for stellar-mass black holes and $\sim 10^4$ G for supermassive black holes [6]. In the force-free regime, where electromagnetic energy density overshadows particle inertia, currents align with magnetic field structures governed by Maxwell's equations in curved spacetime. In denser regions, magnetohydrodynamic (MHD) interactions between fluid motion and currents become significant. Organized currents are also critical for extracting rotational energy from Kerr black holes through the Blandford–Znajek mechanism [7,8], while other mechanisms, such as the magnetic Penrose process, have also been explored [9–11].

The dipolar configuration of electromagnetic fields in magnetized spheres was initially explored in Deutsch's seminal work [12]. General relativistic solutions to Maxwell's equations for the fields of relativistic stars were examined in early studies [13,14], with later research [15–19] focusing on vacuum solutions to assess relativistic corrections in slowly rotating neutron stars. Interior solutions of Maxwell's equations for gravastars were investigated in [20], while oscillations of magnetic and electric fields near relativistic stars were analyzed in [21,22]. Within the braneworld framework, analytical and numerical solutions for magnetized relativistic stars were derived [23–26], with comparisons to pulsar observations yielding upper limits on the tidal charge parameter.

The no-hair theorem states that black holes cannot maintain intrinsic electromagnetic fields, but surrounding plasma or matter can produce them. The dipolar electromagnetic fields generated by a stationary current loop near a Schwarzschild black hole were first studied by Petterson [27], with extensions to Kerr spacetime in subsequent work [28]. Related studies are found in [29–36]. The problem of electromagnetic fields generated by localized sources in curved spacetime has a long and well-established history. Early analytical investigations of a point charge in Schwarzschild spacetime by Cohen and Wald [37] and Hanni and Ruffini [38] demonstrated that the separation of Maxwell's equations naturally leads to multipolar field structures in curved backgrounds. Later studies, including the analysis of black-hole magnetospheres by Ghosh [39], further clarified the role of gravitational curvature in shaping electromagnetic configurations. More recently, Kerner et al. [40] constructed polar magnetic-field solutions in black-hole spacetimes using a separation-of-variables approach and analyzed their multipolar properties. In contrast to these vacuum black-hole geometries, the present work investigates a non-vacuum exponential metric sourced by a scalar field. This modification alters the structure of the radial equation and leads to hypergeometric-type solutions, implying that the dipole moment and near-field magnetic configuration acquire explicit dependence on the exponential metric parameter while preserving the correct flat-spacetime limit. In Schwarzschild geometry, the dipolar vector potential is described using special functions like Legendre and Jacobi polynomials [27], while in flat Minkowski spacetime, the azimuthal potential has a simpler analytical form [41].

Black holes provide an exceptional laboratory for testing gravity in the strong-field regime and for exploring possible observational signatures of modified theories of gravity. In particular, within the Scalar–Tensor–Vector Gravity framework, the presence of a Yukawa-type interaction may alter the spacetime geometry surrounding compact objects. Such modifications can influence the thermodynamic properties of black holes, the dynamics of circular particle motion, and high-energy processes such as particle collisions occurring near the event horizon [42–45]. These theoretical deviations from general relativity can be confronted with observations through several complementary astrophysical probes, including black-hole shadow measurements motivated by Event Horizon Telescope observations, quasinormal-mode spectra, and timing phenomena such as quasi-periodic oscillations that are sensitive to epicyclic motion in strong gravitational fields [46–48].

Gravitational lensing provides another powerful and largely independent tool for probing the underlying spacetime geometry and constraining parameters of alternative gravity models. Lensing phenomena have been extensively studied in both weak and strong regimes, ranging from galaxy-scale surveys such as SLACS to strong gravitational lensing and photon propagation in plasma environments surrounding compact objects [49–52].

Magnetic fields in the environment of compact objects can influence relativistic dynamics in two complementary ways. If the electromagnetic stress–energy is sufficiently strong, it backreacts on the geometry and the system is more appropriately described by exact magnetised black-hole spacetimes rather than by test electromagnetic fields. Prototypical examples are the magnetised Schwarzschild and Kerr configurations constructed by Ernst and by Ernst–Wild [53,54], which embed the black hole into a Melvin magnetic universe. In such Kerr–Melvin backgrounds, global properties – including the existence and extent of ergoregions – depend sensitively on the magnetisation [55]. Moreover, once magnetisation is incorporated at the metric level, integrability may be lost, so that both timelike and null geodesics can become nonintegrable [56–60]. Recently, however, a different exact magnetised Kerr solution was obtained, namely

the Kerr–Bertotti–Robinson spacetime, which describes a Kerr black hole immersed in a Bertotti–Robinson electromagnetic background. Unlike the Kerr–Melvin spacetime, the Kerr–Bertotti–Robinson geometry is of Petrov type D and is supported by a non-aligned, non-null Maxwell field. Dynamically, it also belongs to a different class of spacetimes: timelike geodesics are nonintegrable, whereas null geodesics remain integrable. These results show that strong-field magnetised black-hole spacetimes are not dynamically equivalent and should be distinguished when discussing particle motion and integrability [61,62].

In many astrophysical situations, on the other hand, the field is too weak to appreciably deform the spacetime, yet it can still govern the dynamics of charged particles via the Lorentz force. In this test-field regime, magnetic fields can shift circular-orbit properties and stability boundaries, reshape the phase-space structure of bound and unbound motion, and trigger transitions from regular to chaotic dynamics [63–69]. This motivates accurate long-time integrations in curved spacetimes, where explicit symplectic schemes and adaptive-step implementations provide robust numerical tools for resolving sensitive dynamics [70–74]. Related electromagnetic effects have also been explored in broader settings, including modified-gravity or hairy black-hole backgrounds [75–78].

In this study, we examine the electromagnetic fields produced by a stationary current loop encircling a compact object described by the exponential metric. This metric is an exact non-vacuum solution to Einstein's equations, sourced by a massless scalar field, and serves as a scalar-charged extension of the Schwarzschild solution [79]. Investigating the motion of charged particles in this geometry is significant, as their motion can form static current loops that generate dipolar magnetic fields [80–82].

The structure of the paper is as follows. In Sect. 2, we consider Maxwell equations including the source term in the exponential metric. In Sect. 3 present an analytical solution of Maxwell's equations for the vector potential of the electromagnetic field produced by a stationary current loop in the exponential metric. The conclusions and discussions of the results are summarized in Sect. 5. Throughout the paper, we adopt geometrized units $G = c = 1$ and the spacelike signature $(-,+,+,+)$. Greek indices run from 0 to 3, while Latin indices are restricted to the spatial range 1 to 3.

2 Maxwell equations in exponential metric

Physically, the exponential metric of Ref. [79] may be viewed as representing the gravitational field of a source whose effective potential decreases exponentially with radial distance. In contrast to the Schwarzschild solution, the exponential metric remains regular everywhere for $r > 0$ and, for suitable choices of parameters, may avoid both an event horizon and a curvature singularity. Consequently, it is frequently employed as a toy model for horizonless compact objects and as a framework for probing the robustness of relativistic effects in non-Schwarzschild spacetimes. Historically, exponential metric functions emerged in early alternative gravity approaches and phenomenological models of compact configurations.

To study the electromagnetic fields around compact objects described by the exponential metric, we begin by introducing the line element. The exponential Papapetrou metric takes the form [79]

$$ds^2 = -e^{-\frac{2M}{r}}dt^2 + e^{\frac{2M}{r}}\left(dr^2 + r^2 d\theta^2 + r^2\sin^2\theta d\phi^2\right), \tag{1}$$

where M is a mass of the central object. The determinant of the metric tensor is $g = e^{\frac{4M}{r}} r^4 \sin^2\theta$.

The first pair of Maxwell's equations are

$$\nabla_\mu F^{\mu\nu} = \frac{1}{\sqrt{-g}}\partial_\mu(\sqrt{-g}F^{\mu\nu}) = -4\pi J^\nu, \tag{2}$$

$$\nabla_\mu \tilde{F}^{\mu\nu} = \frac{1}{\sqrt{-g}}\partial_\mu(\sqrt{-g}\tilde{F}^{\mu\nu}) = 0, \tag{3}$$

where $F^{\mu\nu}$ is the electromagnetic tensor, $\tilde{F}^{\mu\nu}$ is its dual, and J^ν represents the four-current density.

For the azimuthal component of the vector potential A_ϕ in the background of the exponential metric (1), the Maxwell equation simplifies to

$$\frac{1}{e^{\frac{2M}{r}} r^2}\partial_r(e^{\frac{2M}{r}} r^2 F^{r\phi}) + \frac{1}{\sin\theta}\partial_\theta(\sin\theta F^{\theta\phi}) = -4\pi J^\phi, \tag{4}$$

where J^ϕ is a source of the electromagnetic field and the components of the Faraday tensor are

$$F^{r\phi} = g^{rr}g^{\phi\phi}F_{r\phi} = \frac{e^{-\frac{4M}{r}}}{r^2\sin^2\theta}\partial_r A_\phi, \tag{5}$$

$$F^{\theta\phi} = g^{\theta\theta}g^{\phi\phi}F_{\theta\phi} = \frac{e^{-\frac{4M}{r}}}{r^4\sin^2\theta}\partial_\theta A_\phi. \tag{6}$$

After simple algebraic manipulations, the Maxwell equation for the vector potential A_ϕ takes the form:

$$r^2 e^{\frac{2M}{r}}\partial_r\left(e^{-\frac{2M}{r}}\partial_r A_\phi\right) + \sin\theta\partial_\theta\left(\frac{1}{\sin\theta}\partial_\theta A_\phi\right) = -4\pi e^{\frac{4M}{r}} r^4\sin^2\theta J^\phi, \tag{7}$$

Let's focus on the source term of the magnetic field generated by the static current loop. According to the Ref. [27],

the total current is determined as

$$I = \int J^{\hat{\phi}} d\hat{r} d\hat{\theta}$$

where hatted quantities are measured in local frame defined as

$$d\hat{t} = e^{-\frac{M}{r}} dt, \tag{8}$$

$$d\hat{r} = e^{\frac{M}{r}} dr, \tag{9}$$

$$d\hat{\theta} = e^{\frac{M}{r}} r d\theta, \tag{10}$$

$$d\hat{\phi} = e^{\frac{M}{r}} r \sin\theta d\phi. \tag{11}$$

Using this formalism, one can show that the azimuthal component of the current density in the global coordinate frame takes the form (See e.g. [27])

$$J^{\phi} = \frac{I}{r^2} e^{-\frac{3M}{r}} \delta(r - r_0)\delta(\cos\theta), \tag{12}$$

where I is the total current flowing in the loop located at a radial coordinate r_0 (with $r_0 = r_{\rm ISCO}$ corresponding to the innermost stable circular orbit of test particle), and $\delta(x)$ is the Dirac delta function ensuring localization of the current distribution.

3 Solution for the vector potential

The solution describing a multipolar magnetic field in the Schwarzschild spacetime was first obtained by Petterson [27]. In his analysis, the Maxwell equations were separated in the Schwarzschild background under the assumption of a stationary, axisymmetric test electromagnetic field. As a result of the separation of variables, the vector potential can be decomposed into radial and angular parts. The radial dependence of the electromagnetic vector potential is governed by a second-order differential equation whose solutions can be expressed in terms of Jacobi polynomials. Meanwhile, the angular dependence is determined by Gegenbauer polynomials, reflecting the underlying spherical symmetry of the Schwarzschild geometry. This decomposition provides a complete set of multipolar magnetic-field configurations around a non-rotating black hole and has since served as a standard framework for studying electromagnetic fields in curved spherically symmetric spacetimes.

To solve the Maxwell equation in the exponential metric with the given current source (12), we expand the vector potential in terms of Legendre polynomials. The general ansatz for A_ϕ is taken as

$$A_\phi = R_L(r) \sin\theta \frac{dP_L(\cos\theta)}{d\theta}, \tag{13}$$

where $P_L(\cos\theta)$ denotes the Legendre polynomial with orbital number L. This form automatically satisfies axisymmetry and ensures the correct parity properties of the magnetic-type vector potential. Substituting the above decomposition into the Maxwell equations reduces the problem to a set of ordinary differential equations for the radial functions $R_L(r)$, which can be solved once the explicit form of the exponential metric and the current distribution are specified. The Legendre polynomial satisfies the well-known differential equation

$$\frac{1}{\sin\theta}\frac{d}{d\theta}\left(\sin\theta \frac{dP_L(\cos\theta)}{d\theta}\right) + L(L+1)P_L(\cos\theta) = 0, \tag{14}$$

and normalized as

$$\int_0^{\pi} d\theta \sin\theta P_L(\cos\theta) P_{L'}(\cos\theta) = \frac{2}{2L+1}\delta_{LL'}. \tag{15}$$

Substituting the ansatz into the Maxwell equation yields the following radial differential equation for $R_L(r)$:

$$\left[r^2 e^{\frac{2M}{r}} \frac{d}{dr}\left(e^{-\frac{2M}{r}} \frac{R_L(r)}{dr}\right) - L(L+1)R_L(r)\right] \times \frac{dP_L(\cos\theta)}{d\theta} = -4\pi I r^2 e^{\frac{M}{r}} \sin\theta \delta(r - r_0)\delta(\cos\theta). \tag{16}$$

For simplicity, we first consider vacuum solution which equivalent to the homogeneous solution for equation above. Hereafter neglecting the source term and performing the simple algebraic manipulations, the radial Eq. (16) can be written as

$$r^2 R_L''(r) + 2M R_L'(r) - L(L+1)R_L(r) = 0. \tag{17}$$

Our calculations show that a solution to the radial equation (17) can be found as

$$R_L(r) = \alpha_L U_L(r) + \beta_L V_L(r), \tag{18}$$

with

$$U_L(r) = \left(-\frac{r}{2M}\right)^{L+1} {}_1F_1\left(-L-1; -2L; \frac{2M}{r}\right),$$
$$V_L(r) = \left(-\frac{2M}{r}\right)^{L} {}_1F_1\left(L; 2L+2; \frac{2M}{r}\right), \tag{19}$$

where ${}_1F_1\,(a, b; c; x)$ is the hypergeometric function, coefficients α_L and β_L are constants of the integration found from the boundary conditions. For simplicity, we first consider the solution for the dipolar configuration of the magnetic field,

which is responsible for $L = 1$. In this case, the radial function becomes

$$R_1(r) = \alpha_1 \left[\frac{r^2}{4M^2}\left(1 + \frac{2M}{r} + \frac{2M^2}{r^2}\right)\right] + \beta_1 \left[\frac{3r^2}{2M^2}\left(1 + \frac{2M}{r} + \frac{2M^2}{r^2} - e^{\frac{2M}{r}}\right)\right]. \quad (20)$$

Boundary conditions play a crucial role in mathematical physics and theoretical astrophysics, as they ensure that the solutions of differential equations have physical meaning. In any physical process or model, such as fields around black holes, the propagation of electromagnetic waves, or the motion of particles, the complete solution can only be obtained by specifying appropriate boundary conditions. These conditions are generally classified into two main types: initial conditions, which specify given values at the beginning of the process in time, for example the initial velocity or position of a particle, and boundary conditions in space, such as the requirement that the field tends to zero at infinity or that smoothness conditions are satisfied at the singularity of the exponential singularity. In astrophysical modeling, for instance when calculating the magnetic field or gravitational potential near black holes, choosing correct boundary conditions guarantees the stability of the solution and its physical interpretation. At the at origin, functions must not diverge, while at spatial infinity they must approach physically expected values. Therefore, in any theoretical analysis, boundary conditions must be included, as they provide consistency between the mathematical model and the physical process. We explicitly impose the matching conditions

$$A_\phi^{(\text{int})}\Big|_{r_0} = A_\phi^{(\text{ext})}\Big|_{r_0}, \qquad \partial_r A_\phi^{(\text{int})}\Big|_{r_0} = \partial_r A_\phi^{(\text{ext})}\Big|_{r_0}. \quad (21)$$

These conditions uniquely fix the remaining integration constants and guarantee smoothness of the vector potential. After imposing these constraints, the solution is fully regular across $r = r_0$. Therefore, the radial function is expressed as

$$R_L(r) = a_L \begin{cases} U_L(r)V_L(r_0), & r \le r_0, \\ U_L(r_0)V_L(r), & r \ge r_0, \end{cases} \quad (22)$$

where a_L is the new unknown coefficient. To find this unknown coefficient let us rewrite Eq. (16) in the following form:

$$\left[\frac{d}{dr}\left(e^{-\frac{2M}{r}}\frac{R_L(r)}{dr}\right) - \frac{L(L+1)}{r^2}e^{-\frac{2M}{r}}R_L(r)\right] \times \frac{dP_L(\cos\theta)}{d\theta} = -4\pi I e^{-\frac{M}{r}} \sin\theta\delta(r - r_0)\delta(\cos\theta), \quad (23)$$

and integrate it near the position of the source r_0. Consequently, one can get

$$a_L \frac{dP_L(\cos\theta)}{d\theta}\frac{R_L(r)}{dr}\Big|_{r_0-\epsilon}^{r_0+\epsilon} = -4\pi I e^{\frac{M}{r_0}} \sin\theta\delta(\cos\theta), \quad (24)$$

where ϵ is an infinitesimal quantity. Simple analyses shows that

$$R_L'(r)\Big|_{r_0-\epsilon}^{r_0+\epsilon} = U_L(r_0)V_L'(r_0) - U_L'(r_0)V_L(r_0) = \frac{2L+1}{2M}e^{\frac{2M}{r_0}}, \quad (25)$$

and equation (24) becomes

$$a_L \frac{2L+1}{2M}\frac{dP_L(\cos\theta)}{d\theta} = -4\pi I e^{-\frac{M}{r_0}} \sin\theta\delta(\cos\theta), \quad (26)$$

By multiplying $\sin\theta dP_{L'}(\cos\theta)/d\theta$ from both sides of the last equation and using the following integral notations:

$$\int_0^\pi d\theta \sin\theta \frac{dP_L(\cos\theta)}{d\theta}\frac{dP_{L'}(\cos\theta)}{d\theta} = \frac{2L'(L'+1)}{2L'+1}\delta_{LL'},$$
$$\int_0^\pi d\theta \sin^2\theta\delta(\cos\theta)\frac{dP_{L'}(\cos\theta)}{d\theta} = P_{L'}'(0), \quad (27)$$

the unknown coefficient a_L can be found as

$$a_L = \frac{4\pi IM}{L(L+1)}P_L'(0)e^{-\frac{M}{r_0}}, \quad (28)$$

$$A_\phi(r,\theta) = 4\pi I e^{-\frac{M}{r_0}}\frac{(2L+1)P_L'(0)}{2L(L+1)} \times \sin\theta\frac{dP_L(\cos\theta)}{d\theta}\begin{cases} U_L(r)V_L(r_0) \\ U_L(r_0)V_L(r) \end{cases}. \quad (29)$$

For simplicity, we first consider the solution for the dipolar configuration of the magnetic field corresponding to $L = 1$. For this particular case the vector potential can be written as

$$A_\phi(r,\theta) = -\frac{3\pi I r_0^2 r^2}{4M^3}e^{-\frac{M}{r_0}}\sin^2\theta \times \begin{cases} \left(1 + \frac{2M}{r} + \frac{2M^2}{r^2}\right)\left(1 + \frac{2M}{r_0} + \frac{2M^2}{r_0^2} - e^{\frac{2M}{r_0}}\right) \\ \left(1 + \frac{2M}{r_0} + \frac{2M^2}{r_0^2}\right)\left(1 + \frac{2M}{r} + \frac{2M^2}{r^2} - e^{\frac{2M}{r}}\right) \end{cases}. \quad (30)$$

Physically, magnetic field lines in axisymmetry coincide with the contour surfaces of $A_\phi = \text{const}$. When A_ϕ itself is constant everywhere, there are no spatial gradients to generate a curl, and hence no magnetic field is present. Such a potential is gauge-trivial and can be removed by a gauge

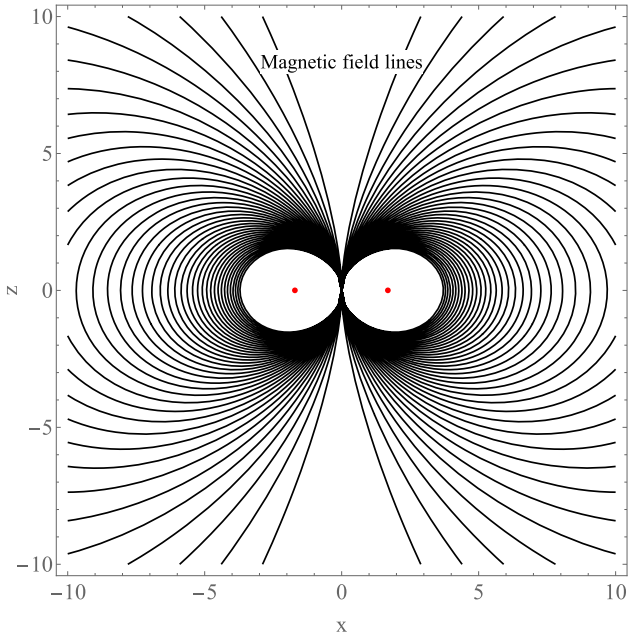

Fig. 1 The magnetic field line in the exponential spacetime. The static current is to be located at $r_0 \simeq 1.7M$

transformation. In Fig. 1 we show magnetic field line in the exponential spacetime.

Interior solution: From Eq. (30), one can easily see that in the interior region of the current loop ($0 \leq r \leq r_0$), the vector potential of dipolar magnetic field can be written in the following form:

$$A_\phi = \frac{1}{2}Br^2\left(1+\frac{2M}{r}+\frac{2M^2}{r^2}\right)\sin^2\theta, \tag{31}$$

where B is the uniform magnetic field measured near the compact object defined as

$$B = -\frac{3\pi I r_0^2}{2M^3}\left(1+\frac{2M}{r_0}+\frac{2M^2}{r_0^2}-e^{\frac{2M}{r_0}}\right)e^{-\frac{M}{r_0}}. \tag{32}$$

The Faraday tensor for the electromagnetic field yields

$$F_{\theta\phi} = B\left(r^2+2Mr+2M^2\right)\sin\theta\cos\theta, \tag{33}$$

$$F_{r\phi} = B(r+M)\sin^2\theta, \tag{34}$$

The components of the magnetic field measured by a proper observer are determined as

$$B^{\hat{r}} = \sqrt{F_{\theta\phi}F^{\theta\phi}} = F_{\theta\phi}\sqrt{g^{\theta\theta}g^{\phi\phi}}, \tag{35}$$

$$B^{\hat{\theta}} = \sqrt{F_{r\phi}F^{r\phi}} = F_{r\phi}\sqrt{g^{rr}g^{\phi\phi}}. \tag{36}$$

and within the stationary current loop they yield

$$B^{\hat{r}} = Be^{-\frac{2M}{r}}\left(1+\frac{2M}{r}+\frac{2M^2}{r^2}\right)\cos\theta, \tag{37}$$

$$B^{\hat{\theta}} = Be^{-\frac{2M}{r}}\left(1+\frac{M}{r}\right)\sin\theta. \tag{38}$$

It is worth emphasizing that the expressions (37) and (38) demonstrate the modification of the dipolar magnetic field structure due to the gravitational field of the compact object. In the flat–spacetime limit ($M \to 0$), one immediately recovers the standard magnetic dipole field inside a circular current loop, i.e.

$$B^{\hat{r}} \to B\cos\theta, \quad B^{\hat{\theta}} \to B\sin\theta,$$

showing the self-consistency of our solution. The additional correction terms proportional to M/r and M^2/r^2 encode the relativistic effects arising from spacetime curvature. These corrections increase in magnitude as one approaches the gravitational radius, indicating that the interior magnetic field is significantly distorted near the compact object.

Furthermore, the exponential redshift factor $e^{-2M/r}$ explicitly accounts for the gravitational suppression of the field as measured by a local observer. This factor ensures that the magnetic field strength decreases as the observer approaches the horizon, which is consistent with the fact that physical measurements in curved spacetime are affected by both frame-dragging and gravitational redshift.

The field structure can also be analyzed in terms of the field-line geometry. Combining (37) and (38), the magnetic field lines satisfy the differential equation

$$\frac{dr}{d\theta} = \frac{B^{\hat{r}}}{B^{\hat{\theta}}} = \frac{\left(1+\frac{2M}{r}+\frac{2M^2}{r^2}\right)}{\left(1+\frac{M}{r}\right)}\cot\theta,$$

which governs the deviation of the field lines from the Newtonian dipole configuration. Far from the compact object ($r \gg M$), this relation reduces to the standard dipolar dependence $r\sin^2\theta = \text{const}$. However, near the origin ($r \sim 0$), the relativistic corrections substantially deform the field-line geometry, leading to more tightly wound and compressed magnetic structures in the polar directions.

Physically, this means that the interior magnetic field generated by the stationary current loop is not only enhanced by curvature effects but also redistributed anisotropically. The radial component $B^{\hat{r}}$ grows faster in the polar regions ($\theta \to 0, \pi$), while the transverse component $B^{\hat{\theta}}$ is amplified near the equatorial plane ($\theta = \pi/2$). Such behavior has direct implications for particle acceleration, plasma confinement, and magnetospheric processes in the vicinity of

compact astrophysical objects such as neutron stars or magnetized black holes.

Exterior solution: Similarly, the vector potential and magnetic field outside the loop can be analyzed.

$$A_\phi = -\frac{3\mu r^2}{4M^3}\left(1+\frac{2M}{r}+\frac{2M^2}{r^2}-e^{\frac{2M}{r}}\right)\sin^2\theta, \tag{39}$$

where μ is a dipole moment of the magnetic field generated by a static current loop in the exponential metric defined as

$$\mu = \pi I e^{-\frac{M}{r_0}} r_0^2\left(1+\frac{2M}{r_0}+\frac{2M^2}{r_0^2}\right).$$

In the proper observer frame, non-vanishing components of the magnetic field exterior region of the current loop $r \geq r_0$ can be calculated by following expressions

$$B^{\hat{r}} = \frac{3\mu}{2M^3}\left[1-\left(1+\frac{2M}{r}+\frac{2M^2}{r^2}\right)e^{-\frac{2M}{r}}\right]\cos\theta, \tag{40}$$

$$B^{\hat{\theta}} = \frac{3\mu}{2M^3}\left[1-\frac{M}{r}-\left(1+\frac{M}{r}\right)e^{-\frac{2M}{r}}\right]\sin\theta, \tag{41}$$

which are results very similar with the expressions for the component of the magnetic field of the relativistic magnetized star in the paper [23], but here the difference is that the dipole moment of the compact object depends on the exponential metric.

It should be emphasized that the expressions (40) and (41) illustrate how the dipolar magnetic field in the exterior region of the current loop is modified by the exponential metric. In the flat–spacetime limit ($M \to 0$), the familiar magnetic dipole field produced by a circular current loop is recovered, namely

$$B^{\hat{r}} = \frac{2\mu}{r^3}\cos\theta, \tag{42}$$

$$B^{\hat{\theta}} = -\frac{\mu}{r^3}\sin\theta, \tag{43}$$

which confirms the consistency of our results. The additional terms proportional to M/r and M^2/r^2 capture the relativistic corrections induced by the curvature of spacetime:

$$B^{\hat{r}} = \frac{2\mu}{r^3}\cos\theta\left[1-\frac{3M}{2r}+\frac{6M^2}{5r^2}+\mathcal{O}\left(M^3/r^3\right)\right], \tag{44}$$

$$B^{\hat{\theta}} = -\frac{\mu}{r^3}\sin\theta\left[1-\frac{M}{r}+\frac{3M^2}{5r^2}+\mathcal{O}\left(M^3/r^3\right)\right]. \tag{45}$$

These relativistic corrections grow more pronounced as one approaches the gravitational radius, implying that the magnetic field becomes increasingly distorted in the vicinity of the compact object.

It is useful to briefly compare our multipolar solution with several standard electromagnetic potentials used in curved spacetime. The general symmetry-based framework underlying self-consistent constructions in the Kerr family is rooted in the global analysis of Carter [83], while the recent discussion by Liu and Wu [84] addresses charged-particle dynamics in combined gravitational and electromagnetic fields, where the electromagnetic structure plays an essential dynamical role. In the present work, by contrast, we adopt the test-field approximation: Maxwell's equations are solved on a fixed exponential background sourced by a scalar field, and the electromagnetic field does not backreact on the metric. We also note that the generalized potential proposed by Azreg-Aïnou [85] is formulated for black-hole spacetimes immersed in an external uniform magnetic field, primarily in rotating settings. Unlike such uniform-field models, our configuration is generated by a localized stationary current loop and therefore naturally yields a dipolar behavior in the exterior region. The exponential metric modifies the radial equation, leading to a hypergeometric-type structure and an explicit dependence of the dipole moment and near-field magnetic configuration on the exponential-metric parameter, while preserving the correct flat-spacetime limit.

4 Charged particle motion

In this section, we investigate the motion of a charged test particle in the exponential spacetime in the presence of an external magnetic field. The dynamics of the particle is described by the Lagrangian

$$\mathscr{L} = \frac{1}{2}m g_{\mu\nu}U^\mu U^\nu + q A_\mu U^\mu, \tag{46}$$

where m and q denote the mass and electric charge of the test particle, respectively. The four–velocity of the particle is defined as $U^\mu = \dot{x}^\mu = dx^\mu/d\tau$, where τ is the proper time along the particle trajectory. The four–velocity satisfies the normalization condition $U_\mu U^\mu = -1$. The equation of motion follows from the Euler–Lagrange equations and takes the covariant form

$$\frac{dU^\mu}{d\tau} + \Gamma^\mu_{\alpha\beta}U^\alpha U^\beta = \frac{q}{m}F^{\mu\nu}U_\nu, \tag{47}$$

where $\Gamma^\mu_{\alpha\beta}$ are the Christoffel symbols associated with the spacetime metric, and $F_{\alpha\beta} = A_{\beta,\alpha} - A_{\alpha,\beta}$ is the electromagnetic field tensor constructed from the four–potential A_μ.

Due to the stationarity and axial symmetry of the spacetime, the motion admits two conserved quantities corresponding to time translations and rotations around the symmetry axis. These constants of motion follow from the gen-

eralized momentum

$$P_\mu = \frac{\partial \mathscr{L}}{\partial U^\mu} = m g_{\mu\nu} U^\nu + q A_\mu. \tag{48}$$

In the exponential spacetime, the conserved quantities in the presence of an external magnetic field can be written as

$$P_t = g_{tt} U^t = -E, \qquad P_\phi = g_{\phi\phi} U^\phi + q A_\phi = L, \tag{49}$$

where E and L represent the total energy and the azimuthal angular momentum of the particle, respectively.

Using the four–potential introduced in Eq. (39), the conserved quantities measured at infinity, namely the specific energy $\mathcal{E} = E/m$ and the specific angular momentum $\mathcal{L} = L/m$, take the form:

$$g_{tt} U^t = -\mathcal{E}, \qquad g_{\phi\phi} U^\phi + \frac{q}{m} A_\phi = \mathcal{L}. \tag{50}$$

These relations demonstrate that the specific energy of the particle remains unaffected by the magnetic field, whereas the specific angular momentum experiences a shift proportional to the electromagnetic interaction term $(q/m)A_\phi$.

Employing the normalization condition of the four–velocity together with Eq. (49), the radial–polar motion of the particle can be written as

$$g_{rr}(U^r)^2 + g_{\theta\theta}(U^\theta)^2 + V(r,\theta) = 0, \tag{51}$$

where the effective potential is defined as

$$V(r,\theta) = 1 + \frac{\mathcal{E}^2}{g_{tt}} + \frac{1}{g_{\phi\phi}}\left(\mathcal{L} - \frac{q}{m} A_\phi\right)^2. \tag{52}$$

For simplicity, we restrict our analysis to particle motion in the equatorial plane, $\theta = \pi/2$, where $U^\theta = 0$. In this case, the radial equation of motion reduces to

$$\dot{r}^2 = \mathcal{E}^2 - V(r), \tag{53}$$

where $V(r)$ is the effective potential defined as

$$V(r) = e^{-\frac{M}{r}} + \left[\frac{\mathcal{L}}{r} + \epsilon\left(r + 2M - r e^{\frac{2M}{r}}\right)\right]^2 e^{-\frac{2M}{r}}, \tag{54}$$

and the dimensionless magnetic parameter ϵ is defined as

$$\epsilon = \frac{3q\mu}{4mM^3}.$$

This parameter can be interpreted as the cyclotron (Larmor) frequency expressed in geometrized units. Equation (53) describes the radial dynamics of a charged particle moving in the exponential gravitational field under the influence of an external magnetic field. Due to the Lorentz force motion of the charged particle is influenced by the external magnetic field. Circular orbits correspond to the extrema of the effective potential and are determined by the conditions $\dot{r} = 0$ and $\ddot{r} = 0$. The stability of circular orbits is determined by the second derivative of the radial potential. The innermost stable circular orbit (ISCO) is defined as the marginally stable orbit separating stable and unstable circular trajectories. The ISCO radius $r_{\rm ISCO}$ is therefore obtained from the conditions $\dot{r} = 0, \ddot{r} = 0$ (corresponding to $V'(r) = 0$) and $V''(r) \geq 0$. Solving this system of equations allows one to determine the specific energy $\mathcal{E}$, the specific angular momentum $\mathcal{L}$, and the radius $r_{\rm ISCO}$ of the marginally stable orbit. The presence of the magnetic field modifies the effective potential through the coupling parameter ϵ, leading to a shift of the ISCO radius compared to the non–magnetized case. In particular, depending on the sign and magnitude of the charge–magnetic field interaction, the ISCO radius can move either closer to or farther from the central compact object, indicating that magnetic effects may significantly influence the dynamics of charged particles in strong gravitational fields.

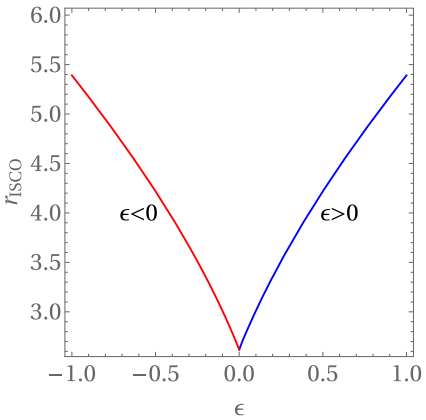

Fig. 2 The dependence of the ISCO position $r_{\rm ISCO}$ from the magnetic parameter ϵ

Our numerical analysis indicates that the presence of an external dipole magnetic field significantly affects the location of the innermost stable circular orbit (ISCO) for charged particles. In particular, the ISCO radius for a charged particle becomes larger than the corresponding value for a neutral particle. This behavior arises from the additional Lorentz force generated by the interaction between the particle's electric charge and the external magnetic field, which effectively modifies the radial force balance governing circular motion.

In Fig. 2, we present the dependence of the ISCO radius, $r_{\rm ISCO}$, on the magnetic interaction parameter ϵ, which characterizes the coupling strength between the particle charge and the magnetic field. As the magnitude of ϵ increases, the ISCO radius shifts outward, indicating that stable circular motion can only occur at larger distances from the compact

object. Physically, this reflects the fact that the magnetic interaction introduces an additional contribution to the effective potential, altering the stability conditions of circular orbits. Another important feature visible in Fig. 2 is the symmetry of the ISCO position under the transformation $\epsilon \to -\epsilon$. This symmetry implies that the ISCO radius depends only on the magnitude of the magnetic interaction parameter rather than its sign. In other words, reversing the direction of the magnetic coupling–equivalently changing the sign of the particle charge or the orientation of the magnetic field–does not affect the radial position of the ISCO, although it may influence the direction of the Lorentz force acting on the particle. To clarify the behavior of the ISCO position, one can analyze the forces acting on a charged particle. In this case, three main contributions must be considered: the gravitational force, the Lorentz force due to the external magnetic field, and the centrifugal force associated with orbital motion. For a stable circular orbit, these forces must balance each other. In the presence of an external magnetic field, the vector potential modifies the conserved angular momentum of the test particle. As a result, the effective centrifugal force is altered. Specifically, the magnetic field can either enhance or oppose the rotational support depending on the charge and field orientation. This modification shifts the equilibrium condition for circular motion. Consequently, the radius at which the balance between gravitational attraction and the combined centrifugal and Lorentz forces is achieved changes. In particular, one finds that the ISCO radius increases in the presence of an external magnetic field, reflecting the additional influence of electromagnetic interaction on the particle's dynamics.

5 Conclusions

In this research, we have investigated the structure of the magnetic field produced by a static current loop in the background of the exponential metric. In particular, we have provided the analytical solution of Maxwell's equations for the vector potential associated with the electromagnetic field generated by charged matter orbiting a compact gravitational object described by this alternative metric. The exponential metric serves as a nontrivial modification of the Schwarzschild spacetime, incorporating the effects of a scalar parameter, and thus allows us to explore the influence of such modifications on electromagnetic processes near compact sources.

We have shown that the angular dependence of the vector potential of the electromagnetic field is expressed in terms of Legendre polynomials, while the radial part is governed by the hypergeometric function of the first kind. The full solution was constructed by imposing appropriate boundary conditions, namely the continuity of the vector potential across the location of the source and the self-consistency of the solution when substituted back into Maxwell's equations. These conditions uniquely determine the integration constants and ensure physical consistency of the field configuration.

Moreover, we have presented the explicit analytical form of the multipole components of the magnetic field, both in the interior and exterior regions of the stationary current loop. In the dipole approximation, the interior magnetic field exhibits a nearly uniform profile, which closely resembles the well-known Wald solution [4] generalized to the exponential metric. In contrast, the exterior magnetic field asymptotically behaves like a dipolar configuration, as expected for localized sources. This distinction highlights how the exponential metric modifies the near-field structure while preserving the classical dipolar decay in the far-field regime.

An important feature we have identified is that the strength of the external magnetic field components is suppressed by the presence of the scalar parameter characterizing the exponential metric. This result stands in sharp contrast to the findings of Ref. [23], where the tidal charge in braneworld scenarios enhances the magnetic field of relativistic magnetized stars. The different roles played by the scalar parameter and the tidal charge underline the sensitivity of electromagnetic fields to the underlying geometry and additional degrees of freedom in alternative theories of gravity.

For compact objects such as black holes, we have also observed that the radius of the innermost stable circular orbit (ISCO) exhibits a pronounced dependence on the scalar parameter, which in turn directly affects the interaction between the electromagnetic field and orbiting matter. This result suggests that astrophysical observables, such as the dynamics of charged or magnetized test particles and the emission properties of accretion disks, may serve as potential probes of deviations from general relativity introduced by exponential-type modifications.

Finally, the obtained vector potential (30) provides a robust foundation for further investigations. In particular, it can be employed to study the dynamics of charged and magnetized particles around compact objects in the exponential metric, the properties of synchrotron and curvature radiation in modified gravity backgrounds, and the possible signatures in accretion and jet-launching processes. These applications would not only deepen our understanding of electromagnetic phenomena in alternative gravitational theories but also open new avenues for confronting such models with astrophysical observations. In summary, the inclusion of a dipole magnetic field modifies the dynamics of charged particles around the compact object and leads to an outward shift of the ISCO radius compared to the neutral case. The numerical results demonstrate that the ISCO position grows with increasing magnetic interaction strength and exhibits a symmetric dependence on the parameter ϵ. This behavior highlights the important role played by electromagnetic fields in determining the structure of particle orbits in strong gravitational environments, which may have potential impli-

cations for astrophysical processes occurring in magnetized compact-object systems.

Funding This research received no external funding. Open access funding provided by SCOAP3.

Data Availability Statement This manuscript has no associated data. [Author's comment: Data sharing not applicable to this article as no datasets were generated or analysed during the current study.]

Code Availability Statement This manuscript has no associated code/software. [Author's comment: Code/Software sharing not applicable to this article as no code/software was generated or analysed during the current study.]

Funded by SCOAP[3].

References

1. K. Akiyama et al., Collaboration Event Horizon Telescope. Astrophys. J. Lett. **910**, L13 (2021). https://doi.org/10.3847/2041-8213/abe4de. arXiv:2105.01173 [astro-ph.HE]
2. M.A. Melvin, Phys. Rev. **139**, B225 (1965). https://doi.org/10.1103/PhysRev.139.B225
3. H. Reissner, Annalen der Physik **355**, 106 (1916) https://doi.org/10.1002/andp.19163550905
4. R.M. Wald, Phys. Rev. D. **10**, 1680 (1974). https://doi.org/10.1103/PhysRevD.10.1680
5. S. L. Shapiro, Phys. Rev. D **95**, 101303 (2017).https://doi.org/10.1103/PhysRevD.95.101303. arXiv:1705.04695 [astro-ph.HE]
6. M. Y. Piotrovich, N. A. Silant'ev, Y. N. Gnedin, T. M. Natsvlishvili (2010)
7. R.D. Blandford, R.L. Znajek, Mon. Not. Roy. Astron. Soc. **179**, 433 (1977). https://doi.org/10.1093/mnras/179.3.433
8. N. Dadhich, (2012). arXiv:1210.1041 [astro-ph.HE]
9. N. Dadhich, A. Tursunov, B. Ahmedov, and Z. Stuchlík, Mon. Not. Roy. Astron. Soc. **478**, L89 (2018).https://doi.org/10.1093/mnrasl/sly073, arXiv:1804.09679 [astro-ph.HE]
10. Z. Stuchlík, M. Kološ, A. Tursunov, Universe **7**, 416 (2021). https://doi.org/10.3390/universe7110416
11. D.P. Viththani, T. Bhanja, V. Patel, P.S. Joshi, Phys. Rev. D **110**, 123035 (2024). https://doi.org/10.1103/PhysRevD.110.123035. arXiv:2407.19738 [gr-qc]
12. A.J. Deutsch, Annales d'Astrophysique **18**, 1 (1955)
13. O. L. M. Ginzburg V. L., Zh. Eksp. Teor. Fiz. **47**, 1030 (1964)
14. J. L. Anderson and J. M. Cohen, **9**, 146 (1970)
15. L. Rezzolla, B.J. Ahmedov, J. C. Miller **322**, 723 (2001). (**astro-ph/0011316**)
16. L. Rezzolla, B.J. Ahmedov, J. C. Miller **31**, 1051 (2001)
17. M. Akramov, C. Trunk, J. Yusupov, and D. Matrasulov, EPL (Europhysics Letters) **147**, 62001 (2024).https://doi.org/10.1209/0295-5075/ad752e. arXiv:2411.14397 [quant-ph]
18. M. Akramov, B. Eshchanov, S. Usanov, S. Norbekov, D. Matrasulov, Phys. Lett. A **524**, 129827 (2024). https://doi.org/10.1016/j.physleta.2024.129827
19. L. Rezzolla, B.J. Ahmedov, J. C. Miller **338**, 816 (2003)
20. B.V. Turimov, B.J. Ahmedov, A. A. Abdujabbarov **24**, 733 (2009). arXiv:0902.0217 [gr-qc]
21. L. Rezzolla and B. J. Ahmedov, **352**, 1161 (2004)
22. L. Rezzolla, B.J. Ahmedov, Mon. Not. Roy. Astron. Soc. **459**, 4144 (2016). https://doi.org/10.1093/mnras/stw864. arXiv:1605.01709 [gr-qc]
23. B.V. Turimov, B.J. Ahmedov, A. A. Hakimov **96**, 104001 (2017)
24. B. J. Ahmedov and F. J. Fattoyev, **78**, 047501 (2008), gr-qc/0608039
25. V. S. Morozova and B. J. Ahmedov, **333**, 133 (2011), 1012.2190 [astro-ph.SR]
26. Z. Asghar, M.F. Shamir, F. Mofarreh, author J. Rayimbaev, O. Sirajiddin, F. Shayimov, Nucl. Phys. B **1024**, 117338 (2026). https://doi.org/10.1016/j.nuclphysb.2026.117338
27. J.A. Petterson, Phys. Rev. D **10**, 3166 (1974). https://doi.org/10.1103/PhysRevD.10.3166
28. J.A. Petterson, Phys. Rev. D **12**, 2218 (1975). https://doi.org/10.1103/PhysRevD.12.2218
29. D.M. Chitre, C.V. Vishveshwara, Phys. Rev. D **12**, 1538 (1975). https://doi.org/10.1103/PhysRevD.12.1538
30. I.G. Moss, Class. Quantum Gravity **28**, 015017 (2011). https://doi.org/10.1088/0264-9381/28/1/015017. arXiv:1102.3022 [gr-qc]
31. D. Pandey, A. Prasad, Progress Theoret. Phys. **68**, 314 (1982). https://doi.org/10.1143/PTP.68.314
32. A.R. King, Phys. Lett. A **56**, 339 (1976). https://doi.org/10.1016/0375-9601(76)90012-2
33. J. Bičák, L. Dvořák, Gen. Relativ. Gravit. **7**, 959 (1976). https://doi.org/10.1007/BF00766413
34. B. Turimov, Int. J. Mod. Phys. D **27**, 1850092 (2018). https://doi.org/10.1142/S021827181850092X
35. S. Rakhmanov, K. Matchonov, H. Yusupov, K. Nasriddinov, D. Matrasulov, European Physical Journal B **98**, 35 (2025). https://doi.org/10.1140/epjb/s10051-025-00885-7
36. S.K. Maurya, A. Errehymy, Z. Umbetova, K. Myrzakulov, I. Ibragimov, A. Dauletov, J. Rayimbaev, JHEAp **47**, 100391 (2025). https://doi.org/10.1016/j.jheap.2025.100391
37. J.M. Cohen, R.M. Wald, J. Math. Phys. **12**, 1845 (1971). https://doi.org/10.1063/1.1665812
38. R.S. Hanni, R. Ruffini, Phys. Rev. D **8**, 3259 (1973). https://doi.org/10.1103/PhysRevD.8.3259
39. P. Ghosh, Mon. Not. Roy. Astron. Soc. **315**, 89 (2000). https://doi.org/10.1046/j.1365-8711.2000.03410.x. arXiv:astro-ph/9907427
40. R. Kerner, G. Koekoek, J. Schuring, J.-W. van Holten, JCAP **03**, 065 (2025). https://doi.org/10.1088/1475-7516/2025/03/065. arXiv:2407.04975 [gr-qc]
41. J. D. Jackson, Classical Electrodynamics, edition 3rd ed. (Wiley, New York, 1999)
42. I. Nishonov, B. Rahmatov, S.U. Khan, M. Zahid, J. Rayimbaev, I. Ibragimov, E. Davletov, Ann. Phys. **486**, 170332 (2026). DOI: https://doi.org/10.1016j.aop.2025.170332
43. M. Zahid, C. Shen, J. Rayimbaev, B. Rahmatov, I. Ibragimov, S. Muminov, M. Umaraliyev, Physics of the Dark Universe 50, 102124 (2025). DOI: https://doi.org/10.1016j.dark.2025.102124
44. S. Saydullayev, I. Nishonov, M. Dusaliyev, O. Xoldorov, S. Murodov, S. Karshiboev, S. Urinov, B. Rahmatov, European Physical Journal C **85**, 1081 (2025). DOI: https://doi.org/10.1140epjcs10052-025-14780-z

45. T. Oteev, J. Rayimbaev, B. Ahmedov, I. Ibragimov, M. Vapayev, S. Muminov, Phys. Dark Univ. **50**, 102118 (2025). DOI: https://doi.org/10.1016/j.dark.2025.102118
46. B. Rahmatov, I. Egamberdiev, O. Umarov, M. Vapayev, S. Karshiboev, Y. Turaev, S. Murodov, Nucl. Phys. B **1022**, 117212 (2026). DOI: https://doi.org/10.1016j.nuclphysb.2025.117212
47. B. Rahmatov, S. Murodov, J. Rayimbaev, S. Muminov, I. Ibragimov, R. Eshburiev, Physics of the Dark Universe **50**, 102102 (2025). DOI: https://doi.org/10.1016j.dark.2025.102102
48. B. Rahmatov, M. Zahid, J. Rayimbaev, R. Rahim, S. Murodov, Chin. J. Phys. **92**, 143 (2024). DOI: https://doi.org/10.1016j.cjph.2024.09.002
49. B. Rahmatov, S. Murodov, J. Rayimbaev, Y. Turaev, I. Egamberdiev, K. Badalov, S. Ahmedov, S. Usanov, Ann. Phys. **488**, 170366 (2026). DOI: https://doi.org/10.1016j.aop.2026.170366
50. B. Rahmatov, I. Egamberdiev, S. Murodov, J. Rayimbaev, I. Ibragimov, E. Davletov, S. Djumanov, Physics of the Dark Universe **50**, 102152 (2025). DOI: https://doi.org/10.1016j.dark.2025.102152
51. B. Rahmatov, I. Nishonov, S. Murodov, I. Egamberdiev, O. Umarov, S. Karshiboev, M. Vapayev, M. Matyoqubov, Phys. Dark Univ. **52**, 102253 (2026). DOI: https://doi.org/10.1016/j.dark.2026.102253
52. L. Meliyeva, O. Xoldorov, O. Tursunboyev, S. Karshiboev, S. Murodov, I. Nishonov, B. Rahmatov, Chin. Phys. C **49**, 125102 (2025). DOI: https://doi.org/10.10881674-1137adf4a0
53. F.J. Ernst, J. Math. Phys. **17**, 54 (1976). https://doi.org/10.1063/1.522781
54. F.J. Ernst, W.J. Wild, J. Math. Phys. **17**, 182 (1976). https://doi.org/10.1063/1.522875
55. G.W. Gibbons, A.H. Mujtaba, C.N. Pope, Class. Quant. Grav. **30**, 125008 (2013). https://doi.org/10.1088/0264-9381/30/12/125008. arXiv:1301.3927 [gr-qc]
56. R.B. Mann, Gen. Rel. Grav. **24**, 433 (1992). https://doi.org/10.1007/BF00760418
57. D. Li, X. Wu, Eur. Phys. J. Plus **134**, 96 (2019). https://doi.org/10.1140/epjp/i2019-12502-9. arXiv:1803.02119 [gr-qc]
58. D. Yang, W. Liu, X. Wu, Eur. Phys. J. C **83**, 357 (2023). https://doi.org/10.1140/epjc/s10052-023-11551-6. arXiv:2305.02702 [gr-qc]
59. D. Yang, X. Wu, Eur. Phys. J. C **83**, 789 (2023). https://doi.org/10.1140/epjc/s10052-023-11978-x
60. C. Liu, D. Yang, X. Wu, Eur. Phys. J. C **85**, 104 (2025). https://doi.org/10.1140/epjc/s10052-025-13776-z
61. J. Podolsky, H. Ovcharenko, Phys. Rev. Lett. **135**, 181401 (2025). https://doi.org/10.1103/rfgv-ybz5. arXiv:2507.05199 [gr-qc]
62. J. Lu, X. Wu, Eur. Phys. J. C **86**, 256 (2026). https://doi.org/10.1140/epjc/s10052-026-15482-w. arXiv:2603.12674 [gr-qc]
63. M. Takahashi, H. Koyama, Astrophys. J. **693**, 472 (2009). https://doi.org/10.1088/0004-637X/693/1/472. arXiv:0807.0277 [astro-ph]
64. O. Kopacek, V. Karas, J. Kovar, Z. Stuchlik, Astrophys. J. **722**, 1240 (2010). https://doi.org/10.1088/0004-637X/722/2/1240. arXiv:1008.4650 [astro-ph.HE]
65. O. Kopáček, V. Karas, Astrophys. J. **787**, 117 (2014). https://doi.org/10.1088/0004-637X/787/2/117. arXiv:1404.5495 [astro-ph.HE]
66. O. Kopáček, V. Karas, Astrophys. J. **853**, 53 (2018). https://doi.org/10.3847/1538-4357/aaa45f. arXiv:1801.01576 [astro-ph.HE]
67. R. Pánis, M. Kološ, Z. Stuchlík, Eur. Phys. J. C **79**, 479 (2019). https://doi.org/10.1140/epjc/s10052-019-6961-7. arXiv:1905.01186 [gr-qc]
68. K. Schroven, S. Grunau, Phys. Rev. D **103**, 024016 (2021). https://doi.org/10.1103/PhysRevD.103.024016. arXiv:2007.08823 [gr-qc]
69. W. Cao, W. Liu, X. Wu, Phys. Rev. D **105**, 124039 (2022). https://doi.org/10.1103/PhysRevD.105.124039. arXiv:2206.09518 [gr-qc]
70. Y. Wang, W. Sun, F. Liu, X. Wu, Astrophys. J. **907**, 66 (2021). https://doi.org/10.3847/1538-4357/abcb8d. arXiv:2102.00373 [gr-qc]
71. Y. Wang, W. Sun, F. Liu, X. Wu, Astrophys. J. **909**, 22 (2021). https://doi.org/10.3847/1538-4357/abd701. arXiv:2103.02864 [gr-qc]
72. Y. Wang, W. Sun, F. Liu, X. Wu, Astrophys. J. Suppl. **254**, 8 (2021). https://doi.org/10.3847/1538-4365/abf116. arXiv:2103.12272 [gr-qc]
73. W. Sun, Y. Wang, F. Liu, X. Wu, Eur. Phys. J. C **81**, 785 (2021). https://doi.org/10.1140/epjc/s10052-021-09579-7. arXiv:2109.02295 [gr-qc]
74. X. Wu, Y. Wang, W. Sun, F. Liu, D. Ma, Astrophys. J. Suppl. **275**, 31 (2024). https://doi.org/10.3847/1538-4365/ad8351. arXiv:2412.01045 [gr-qc]
75. W. Cao, X. Wu, J. Lyu, Eur. Phys. J. C **84**, 435 (2024). https://doi.org/10.1140/epjc/s10052-024-12804-8. arXiv:2404.19225 [gr-qc]
76. Z. Stuchlík, J. Vrba, M. Kološ, A. Tursunov, JHEAp **44**, 500 (2024). https://doi.org/10.1016/j.jheap.2024.11.006. arXiv:2412.04996 [astro-ph.HE]
77. B. Rahmatov, B. Turimov, S. Murodov, K. Khaknazarova, S. Usanov, M. Vapayev, Z. Avezmuratova, Nucl. Phys. B **1024**, 117344 (2026). https://doi.org/10.1016/j.nuclphysb.2026.117344
78. J. Lu, X. Wu, Eur. Phys. J. C **85**, 1122 (2025). https://doi.org/10.1140/epjc/s10052-025-14853-z. arXiv:2510.08954 [gr-qc]
79. A. Papapetrou, Z. Phys. **139**, 518 (1954). https://doi.org/10.1007/BF01374560
80. B. Turimov, A. Davlataliev, A. Abdujabbarov, B. Ahmedov, Phys. Rev. D **110**, 084053 (2024). https://doi.org/10.1103/PhysRevD.110.084053. arXiv:2409.06225 [gr-qc]
81. B. Turimov, K. Karshiboev, A. Abdujabbarov, S. Mitra, and S. Karshiboev, Galaxies **12** (2024).https://doi.org/10.3390/galaxies12050058
82. B. Turimov, Y. Turaev, B. Ahmedov, Z. Stuchlík, Phys. Dark Univ. **35**, 100946 (2022). https://doi.org/10.1016/j.dark.2021.100946
83. B. Carter, Phys. Rev. **174**, 1559 (1968). https://doi.org/10.1103/PhysRev.174.1559
84. C. Liu, X. Wu, Phys. Lett. B **867**, 139616 (2025). https://doi.org/10.1016/j.physletb.2025.139616
85. M. Azreg-Aïnou, Eur. Phys. J. C **76**, 414 (2016). https://doi.org/10.1140/epjc/s10052-016-4259-6. arXiv:1603.07894 [gr-qc]